

549-34
82214

LOW-DIMENSIONAL DYNAMICAL MODELS OF THERMAL CONVECTION

A. Liakopoulos
Department of Mechanical Engineering and Mechanics
Lehigh University
Bethlehem, Pennsylvania, 18015

60

ABSTRACT

A low-dimensional dynamical model for transitional buoyancy-driven flow in a differentially heated tall enclosure is presented. The full governing partial differential equations with the associated boundary conditions are solved by a spectral element method for a cavity of aspect ratio $A = 20$. Proper orthogonal decomposition is applied to the oscillatory solution at Prandtl number $Pr = Pr_o = 0.71$ and Grashof number $Gr = Gr_o = 3.2 \times 10^4$ to construct empirical eigenfunctions. Using the four most energetic empirical eigenfunctions for the velocity and temperature as basis functions and applying Galerkin's method, a reduced model consisting of eight nonlinear ordinary differential equations is obtained. Close to the "design" conditions (Pr_o, Gr_o) , the low-order model (LOM) predictions are in excellent agreement with the predictions of the full model. In particular, the critical Grashof number at the onset of the first temporal flow instability (Hopf bifurcation) as well as the frequency and amplitude of oscillations at supercritical conditions are in excellent agreement with the predictions of the full model. Far from the "design" conditions, the LOM predicts the existence of multiple stable steady solutions at large values of Gr , and a unique stable steady solution at small values of Gr , and exhibits hysteretic behavior that is qualitatively similar to that observed in direct numerical simulations based on the full model.

INTRODUCTION

Thermally driven cavity flows provide a wealth of paradigms for the study of flow instabilities and transition to turbulence. A classical problem is concerned with the motion in a rectangular cavity when the vertical boundaries are maintained at fixed but distinct temperatures and the upper and lower horizontal surfaces are adiabatic. For a Newtonian fluid, subject to the Boussinesq approximation, the flow field is governed by three dimensionless parameters: the aspect ratio A (height/width), the Prandtl number Pr , and the Grashof number Gr (based on the cavity width). At moderate Gr , the base flow corresponds to a single unicellular state. As Gr increases, both time-dependent and stationary bifurcations can occur, depending on the aspect ratio and Prandtl number. In the present study we investigate the possibility of developing low-dimensional dynamical models of oscillatory multicellular convection in a rectangular cavity of aspect ratio $A = 20$.

The method of weighted residuals can be used to transform evolution partial differential equations (PDEs) to systems of ordinary differential equations (ODEs). Most frequently, trigonometric or orthogonal polynomials are used as basis functions (e.g., Gottlieb and Orszag, 1977). Other basis functions, e.g., spline functions (Liakopoulos, 1985, Liakopoulos and Hsu, 1984) have also been used successfully. In practice, the infinite dimensional problem is truncated to a finite dimensional space of dimension n . To ensure that the dynamic behavior described by the resulting finite dimensional system converges to that of the original infinite dimensional problem, the required dimension n is typically high. A large reduction in the dimension of the resulting system of ODEs is accomplished by expanding the unknown functions in terms of basis functions that are constructed specifically for each flow system and reflect the behavior of the flow in the vicinity of some values of the controlling parameters. Proper Orthogonal Decomposition (POD) is a rigorous methodology for obtaining a set of optimal basis functions (Berkooz et al., 1993). POD systematically identifies the most energetic eigenmodes that contain enough information for accurate description of the flow dynamics. Consequently, one is able to compress numerical or experimental data by retaining a small number of modes that capture most of the flow and temperature "energy".

In this paper, we consider the buoyancy-driven flow in a laterally heated enclosure of aspect ratio $A = 20$. Direct numerical simulations are performed for $Pr = 0.71$ and $10^3 \leq Gr \leq 10^5$. Proper Orthogonal Decomposition and Galerkin's version of the method of weighted residuals are employed to derive low-order dynamical models of the flow in the transitional regime.

FULL MODEL

The flow domain consists of a two-dimensional rectangular cavity in which the upper and lower surfaces are adiabatic and the vertical walls are maintained at constant but different temperatures. Subject to the Boussinesq approximation, the continuity, momentum, and energy equations are written in dimensionless form:

$$\nabla \cdot \vec{V} = 0, \quad (1)$$

$$\frac{\partial \vec{V}}{\partial t} + (\vec{V} \cdot \nabla) \vec{V} + \nabla P = \Theta \vec{j} + \frac{1}{\sqrt{Gr}} \nabla^2 \vec{V} \quad (2)$$

$$\frac{\partial \Theta}{\partial t} + \vec{V} \cdot \nabla \Theta = \frac{1}{Pr \sqrt{Gr}} \nabla^2 \Theta \quad (3)$$

with boundary conditions $\vec{V} = 0$ along the walls, $\Theta(x = 0, y) = 1$, $\Theta(x = 1, y) = 0$, and $\frac{\partial \Theta}{\partial y}(x, \pm \frac{A}{2}) = 0$. The dimensionless variables are defined as

$$(x, y) = (x^*, y^*)/l, \quad t = \frac{u_c}{l} t^*, \quad \vec{V} = \frac{\vec{V}^*}{u_c} \quad (4)$$

$$P = \frac{p^*}{\rho u_c^2}, \quad \text{and} \quad \Theta = \frac{T - T_1}{T_2 - T_1}.$$

Here T_1 and T_2 are the cold and hot wall temperatures, respectively, l is the cavity width, $Pr = \nu/\alpha$ is the Prandtl number, $Gr = \frac{\beta g (T_2 - T_1) l^3}{\nu^2}$ is the Grashof number, ν is the kinematic viscosity, α is the thermal diffusivity, β is the thermal expansion coefficient, g is the acceleration of gravity, \vec{j} is the unit vector in the direction opposite to gravity, and $u_c = \sqrt{\beta g l (T_2 - T_1)}$. Note that the characteristic velocity u_c has been determined by balancing the inertia and buoyancy forces in the momentum equation and the pressure has been scaled by two times the dynamic pressure. These are appropriate scales for the high Grashof number thermal convection considered in the present study.

For high Gr the IBVP (full model) has multiple stable solutions that can be computed by assigning appropriate initial conditions. For example, if we start with a three-cell time-independent solution at $Gr = 4 \times 10^4$ and gradually decrease Gr , different solution branches can be reached. At $Gr = 3.2 \times 10^4$, a stable three-cell time-independent solution is found. This contrasts the four-cell time-dependent flow that is found when Gr is gradually increased. Reducing Gr further, we obtain a sequence of time-independent solutions that may belong to the same steady solution branch. At $Gr = 10^4$ a steady multicellular solution is computed. Note that the multiplicity of solutions is a property of the full model for large values of Gr only. At $Gr = 5 \times 10^3$, the solution to the IBVP computed by decreasing Gr is identical to the one computed for increasing Gr . We have found no evidence of multiple solutions as Gr was decreased further. Although an exhaustive search for all possible solutions is prohibitively expensive, we may conclude with a reasonable degree of confidence that the full model has a unique stable steady solution for $Gr \leq 8 \times 10^3$.

DERIVATION OF THE LOW-ORDER MODEL

In the context of transitional thermal convection, we assume that, for some values (Pr_o, Gr_o) , we have obtained spontaneously oscillatory flow and temperature fields. We refer to these values of the parameters as “design” parameters or “design” conditions. Furthermore, it is assumed that M snapshots of each field have been experimentally measured or computed based on the full model for $Pr = Pr_o$ and $Gr = Gr_o$. Following the procedure described in Liakopoulos and Gunes (1996), we construct the stationary empirical eigenfunctions. Expanding the unknown functions in terms of the eigenfunctions, applying Galerkin method, and making use of the orthonormality property of the empirical eigenfunctions, we obtain a system of non-linear ODEs for the temporal expansion coefficients

$$\begin{aligned} \frac{da_k}{dt} &= A_k + \frac{1}{\sqrt{Gr}} B_k + C_{ki} a_i + \frac{1}{\sqrt{Gr}} D_{ki} a_i + E_{kij} a_i a_j + R_{ki} b_i \\ \frac{db_k}{dt} &= F_k + \frac{1}{Pr\sqrt{Gr}} G_k + H_{ki} a_i + \frac{1}{Pr\sqrt{Gr}} I_{ki} b_i + J_{kij} a_i b_j + K_{ki} b_i. \end{aligned} \quad (5)$$

EIGENVALUES AND EMPIRICAL EIGENFUNCTIONS

Twenty snapshots ($M = 20$) of the oscillatory solution for $Gr = Gr_o = 3.2 \times 10^4$ and $Pr = Pr_o = 0.71$ provide the input data for the extraction of the empirical eigenfunctions. A list of the eight largest eigenvalues is given in Table I. The eigenvalues have been normalized so that their sum equals unity, and their cumulative contribution to the total flow and temperature fluctuation “energy” is given in the last column of Tables Ia and Ib, respectively. The first four eigenmodes capture 99.83% of both flow and temperature fluctuation “energy”. However, the energy distribution among the four most energetic modes is slightly different for temperature than for velocity. The principal eigenvalue contributes 63.07% of the total fluctuation “energy” for temperature as opposed to 55.83% for velocity. Furthermore, for the temperature eigenvalues $\lambda_2 \approx \lambda_1/2$ and $\lambda_4 \approx \lambda_3/2$.

Isotherms and streamlines for the four most energetic empirical eigenfunctions are shown in Figure 1. Note that although the direct numerical simulations and the proper orthogonal decomposition are performed in terms of primitive variables (u, v, P, Θ) , the velocity eigenfunctions are presented here in terms of the corresponding streamfunction. The velocity and temperature eigenfunctions are both centro-symmetric. The two most energetic eigenfunctions are localized in the central part of the cavity where velocity and temperature fluctuations are most vigorous. Higher order eigenfunctions capture features in the entire cavity, including regions close to the horizontal end walls. Repeated flow and temperature structures can be seen in the middle part of the cavity. These repeated structures form patterns that are characteristic of the early transition process of convection in laterally heated tall cavities. Preliminary results reveal that the most energetic eigenmodes exhibit the same spatial patterns in the middle part of a cavity of aspect ratio $A = 40$.

RESULTS BASED ON THE LOW-ORDER MODEL

In developing a reduced model, it is desired to keep the dimensionality of the system sufficiently low so that the methods of the dynamical systems theory can be effectively applied. On the other hand, enough modes should be retained so that the field variables are reconstructed accurately, most of the flow and temperature fluctuation “energy” is captured, and the potentially important information hidden in the small scale features of higher modes is not lost. For the problem at hand, at least four modes for each field variable need to be retained in order to obtain oscillations of correct amplitude at “design” conditions (Gr_o, Pr_o) . Retaining fewer than four modes leads to unrealistically large modal amplitudes. The results summarized below are obtained using eight ODEs (four from the momentum equation and four from the energy equation). The critical points (fixed points, steady solutions) of the low-order model are found by setting the

right hand side of equation (5) to zero and solving the resulting nonlinear algebraic equations. The stability of a steady solution is then determined by the eigenvalues of the associated Jacobian matrix evaluated at the critical point under consideration. Note that the Jacobian matrix is real and non-symmetric. Several steady solution branches are found for $1 \leq Gr \leq 2 \times 10^5$ using a Newton-Raphson method with random initial guesses for the solution components. For $Gr < 2.63 \times 10^4$, a unique branch of stable fixed points is found. We refer to this branch as the primary solution branch. It is denoted by A in Figure 2 where the norm $(a_i a_i + b_i b_i)^{1/2}$ of the fixed points is plotted against Gr . For $Gr \geq 2.63 \times 10^4$, multiple steady solutions are found. Since we are interested in solutions that are potentially relevant to the solutions of the original system of PDEs, we discard fixed points whose norm is several orders of magnitude larger than the norm of the primary branch. In Figure 2, we present only fixed points with a norm smaller than 3 in the range $1 \leq Gr \leq 10^5$. Thick lines represent stable fixed points while thin lines correspond to unstable fixed points. Two stable steady solutions exist for $2.63 \times 10^4 \leq Gr \leq 3.11 \times 10^4$. At $Gr = 3.11 \times 10^4$, the fixed point on the primary branch undergoes a Hopf bifurcation that marks the onset of periodic oscillations in time. For $3.11 \times 10^4 \leq Gr \leq 4.14 \times 10^4$, we find one stable steady solution (branch B) while for $4.14 \times 10^4 \leq Gr \leq 9.87 \times 10^4$, two stable steady solutions exist (branches B and C). The fixed point along branch C becomes unstable at $Gr = 9.87 \times 10^4$. For $Gr > 9.87 \times 10^4$, we find only one stable steady solution that maintains its stability at least up to $Gr = 2 \times 10^5$. These stability results have been confirmed by solving equations (5) with suitable initial conditions using a fourth order Runge-Kutta ODE solver.

A detailed quantitative comparison of the low-order model predictions with the full model is beyond the scope of the present work. However, we mention some encouraging observations both quantitative and qualitative in nature. The low-order model prediction of a Hopf bifurcation along the primary branch is in excellent agreement with the full model prediction. The low-order model predicts a Hopf bifurcation at $Gr = Gr_H = 3.11 \times 10^4$, while the full model predicts the onset of spontaneously oscillatory convection at $Gr \simeq 3.1 \times 10^4$. The frequency of oscillations at the onset of the temporal instability is successfully predicted by the low-order model. Turning our attention to values of Gr far from the design conditions, we find qualitative agreement between the low-order model and the full model. For example, the low-order model predicts a stationary bifurcation at $Gr < Gr_H$ in qualitative agreement with the full model which predicts that a stationary instability certainly precedes the onset of oscillatory convection for $A = 20$ and $Pr = 0.71$. The low-order model predicts a unique stable steady solution for small values of Gr and multiple stable steady solutions for large values of Gr in agreement with the direct numerical simulation results based on the full model. However, the critical values of Gr at which the multiple stable solutions emerge or lose their stability are at variance with the PDE-based calculations. More research is needed in documenting the multiplicity of solutions of the PDEs before a meaningful quantitative comparison with the ODE predictions can be accomplished. This is a demanding task since direct numerical studies based on the full model are computationally intensive and are complicated by the presence of hysteresis effects.

CONCLUSIONS

A low-dimensional dynamical model for transitional buoyancy-driven flow in a differentially heated enclosure of aspect ratio $A=20$ has been presented. Empirical eigenfunctions have been determined by applying the snapshot version of the proper orthogonal decomposition at "design" conditions $Pr_o = 0.71$ and $Gr_o = 3.2 \times 10^4$. The computed eigenfunctions are centro-symmetric. Using the four most energetic eigenmodes of the velocity field and the four most energetic eigenmodes of the temperature field, a Galerkin procedure leads to an eight-equation nonlinear dynamical model. Close to the "design" conditions, the low-order model predictions are in excellent agreement with the predictions of the full model. Conditions at the onset of the first temporal instability (Hopf bifurcation) of the flow are in excellent agreement with the full model predictions in terms of the critical Grashof number, the frequency of oscillations, and the amplitude

of oscillations at supercritical conditions. Far from the "design" conditions, the LOM predicts a unique steady solution at small values of Gr , and multiple stable steady solutions at large values of Gr , and exhibits hysteretic behavior that is qualitatively similar to that observed in direct numerical simulations based on the full model. It is believed that low-order models have the potential of becoming a viable tool in the study of complex transitional flows. Note, however, that the governing equations have been scaled appropriately in order to widen the range of applicability of the resulting low-order model. The possibility of improving the performance of the LOM by constructing empirical eigenfunctions that take into account the behavior of the flow system at multiple values of Gr is under investigation.

ACKNOWLEDGMENT

This work was partially supported by NASA /LeRC under contract No. NAG3-1632.

REFERENCES

Berkooz, G., P. Holmes, and J. L. Lumley (1993), "The Proper Orthogonal Decomposition in the Analysis of Turbulent Flows," *Ann. Rev. Fluid Mech.* 25, 539-575.

Gottlieb, D. and S. A. Orszag (1977), "Numerical Analysis of Spectral Methods," Society for Industrial and Applied Mathematics, Philadelphia, PA.

Liakopoulos, A. and Gunes, H. (1996), "Low-Dimensional Description of Oscillatory Thermal Convection: The Small Prandtl Number Limit," submitted, *Theoretical and Computational Fluid Mechanics*.

Liakopoulos, A. (1985), "Computation of High Speed Turbulent Boundary Layer Flows Using the $k-\epsilon$ Turbulence Model," *Int. J. Num. Meth. Fluids.* 5, No. 1, 81-97.

Liakopoulos, A. and C. C. Hsu (1984), "On a Class of Compressible Laminar Boundary-Layer Flows and the Solution Behavior Near Separation," *J. Fluid Mech.* 149, 339-353.

Lumley, J. L. (1967), "The Structure of Inhomogeneous Turbulent Flows," In *Atmospheric Turbulence and Radio Wave Propagation*, A. M. Yaglom and V. I. Tatarski, ed. 166-178 (Nauka, Moscow).

Table I

a) Velocity eigenvalues

Modes	Normalized Eigenvalue	Cumulative Energy Contribution (%)
1	0.5583	55.83
2	0.3424	90.07
3	0.0658	96.65
4	0.0317	99.83
5	0.921×10^{-3}	99.92
6	0.707×10^{-3}	99.99
7	0.603×10^{-4}	99.99
8	0.293×10^{-4}	100.0

b) Temperature eigenvalues

Modes	Normalized Eigenvalue	Cumulative Energy Contribution (%)
1	0.6307	63.07
2	0.3163	94.70
3	0.0345	98.15
4	0.0168	99.83
5	0.881×10^{-3}	99.92
6	0.677×10^{-3}	99.99
7	0.696×10^{-4}	99.99
8	0.524×10^{-4}	100.0

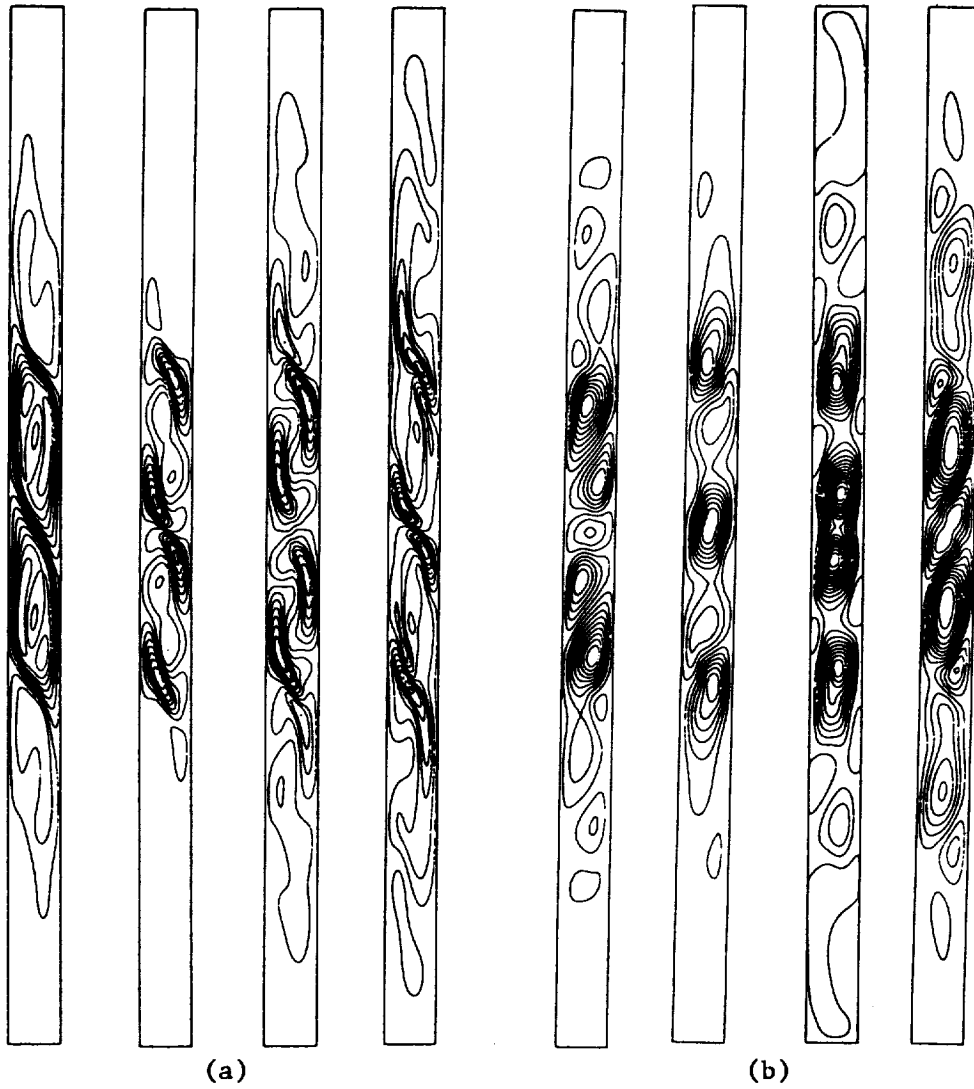


Figure 1. Temperature (a) and velocity (b) empirical eigenfunctions.

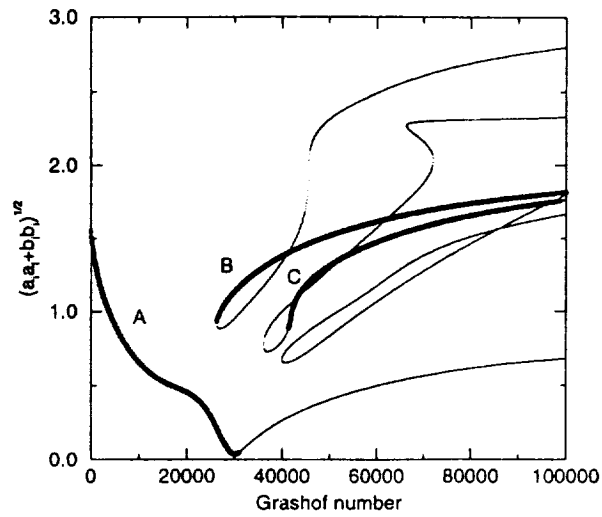


Figure 2. Fixed points of the LOM and their stability. $Pr = 0.71$.